Acta Mech 228, 2541–2554 (2017)
DOI 10.1007/s00707-017-1840-5

ORIGINAL PAPER

Jianfeng Zhao · Jinlin Liu · Guozheng Kang · Linan An · Xu Zhang

The competitive nucleation of misfit dislocation dipole and misfit extended dislocation dipole in nanocomposites

Received: 21 September 2016 / Published online: 11 April 2017

Abstract Nanocomposites have shown excellent mechanical and physical properties; however, their properties are seriously affected by the nucleation of misfit defects at the interfaces between the inclusion and the matrix. Based on the energy rule, the nucleation criteria for a misfit extended dislocation dipole (MEDD) and a misfit screw dislocation dipole (MSDD) are analytically given. Furthermore, we systematically investigate the effects of the geometrical and mechanical factors, such as the radius of the inclusion, the misfit strain, the shear modulus ratio and the stacking fault energy, on the competitive nucleation between MEDD and MSDD. It is found that the stacking fault energy has a decisive effect on the competitive nucleation of MEDD and MSDD. The critical stacking fault energy for the nucleation transferring from MSDD to MEDD increases with the increase of the shear modulus ratio and decrease of the misfit strain, while it is almost not affected by the inclusion radius.

1 Introduction

Nanocomposites have been widely studied and used due to their excellent mechanical and physical properties [1,2]. Meanwhile, their microstructure can be manipulated by adjusting the characteristics of the inclusion and matrix to optimize their performance. However, the misfit stress, which results from the misfit of the crystal lattices between the inclusion and matrix, seriously influences the properties of the nanocomposites. The misfit stress can be partially relaxed by the formation of misfit defects at the phase interfaces [3–9]. Thus, it is desired to understand the mechanism and the critical condition for the nucleation of misfit defects.

The nucleated misfit dislocations usually act as the source for the initiation of damage and crack. A lot of researches have focused on the nucleation of various dislocation configurations at or near phase boundary in different materials, such as misfit dislocations and misfit dislocation dipole in nanowires composites [10–14], misfit dislocation loop in nanocomposites with dilatational inclusions as quantum dots or wires [15] and misfit dislocation dipole in core/shell nanowires [8,16]. Generally, the interface is treated as perfect and classical theory of elasticity is employed in the aforementioned publications. In recent years, it has been claimed that the surface/interface effects also played a role if the inclusion size is on the order of nanometer and the interface-to-bulk ratio is significant [17–20] or the interface is imperfect [21–26]; great effort has been made by researchers to tackle this kind of problems with the Gurtin–Murdoch model (namely, surface/interface stress

J. Zhao · J. Liu · G. Kang · X. Zhang (✉)
School of Mechanics and Engineering, Southwest Jiaotong University, Chengdu 610031, China
E-mail: xuzhang85@126.com

L. An
Department of Materials Science and Engineering, University of Central Florida, Orlando, FL 32733, USA

X. Zhang
State Key Laboratory of Nonlinear Mechanics, Institute of Mechanics, Chinese Academy of Sciences, Beijing 100190, China

model) [27–33]. For conducting a systematic research, the interface effect will be considered in the subsequent work, and in this paper, a perfect interface is employed to make the first effort.

Theoretically, the dislocations can exist as extended dislocations (or partial dislocations) in materials according to Frank's energy criterion [34]. In nanocomposites, it has also been experimentally observed that once a full misfit dislocation is formed, it would dissociate into two partials which then split further from each other to form a stacking fault (SF) [9]. The formed stacking faults can easily rearrange to nucleate embryonic twins; then, these nuclei may coalesce to form twins during further deformation. Introducing nanoscale twins into the material is a sophisticated strengthening method, which can improve the strength without compromising ductility [35–38]. Thus, twins in nanocomposites will not only release the stress concentration, but also accommodate further deformation and thus enhance the strength and ductility of the nanocomposites [9]. The desired microstructure of twin is easier to form in materials with lower SF energy, where a wider SF ribbon required to connect the two dissociated partial dislocations may eventually trigger the nucleation of twin [39]. Therefore, it is very important to understand the nucleation mechanism of extended dislocations in nanocomposites. However, comparing to the great effort for the nucleation of misfit dislocations in nanocomposites, the misfit dislocations nucleated as partial dislocations in nanocomposites were rarely reported [7,9,40].

In nanocrystalline materials, it has been found that there is a competition between the nucleation of full and partial dislocations (related to SF) [41,42]. However, there is no comprehensive study to reveal such competition in nanocomposites. Considering the fact that the nucleation of these two different kinds of defects could lead to contrary effect on the mechanical performance of materials, in this paper, we devote to investigate the competition mechanism for the energetically favorable nucleation of these two defects, which accompanies the relaxation of misfit stress due to the lattice misfit between the inclusion and the matrix with classical theory of elasticity. For the purpose of illustrating the main features of the nucleation of misfit dislocation dipole due to the misfit strain at the interface, and of avoiding the complicated mathematical description, screw dislocation dipole is chosen to be investigated here. Specifically, the influences of some parameters, such as the radius of the inclusion, the misfit strain, the shear modulus ratio of the inclusion to the matrix and the SF energy on the competitive nucleation of these two defects, are investigated in detail.

The paper is organized as follows: Firstly, the nucleation of an MSDD is reviewed. Then, the energetically favorable nucleation criterion of an MEDD and the related equilibrium separation of the SF ribbon are studied, accompanying the systematically analysis of the influence of the material parameters. Finally, we discuss the competitive nucleation between the MEDD and MSDD.

2 Nucleation of a MSDD

It has been revealed that the nucleation of misfit dislocation dipoles is more favorable than misfit dislocations because the energy barrier for nucleating a misfit dislocation dipole is lower in wire composites [16]. The specifically analyzed nanocomposite is idealized as an infinite matrix containing a buried strained cylindrical inclusion for simplification, which can be treated as a two-dimensional problem. Generally, the dislocation should nucleate at preferred location where the whole energy of the system is at its minimum. However, considering the fact that preferred location of the MEDD discussed below will be affected by two nonlinear coupled parameters, i.e., the distance of the MEDD from the interface and the separation of the two extended partials, brings great challenge for computation. Thus, the investigated configuration is simplified for an MSDD with its two constituents located at the phase interface $x = R$ and $x' = -R$, where R is the radius of the inclusion, as shown in Fig. 1. Future work will focus on the real situation of dislocation with preferred location and then compare with the results in this paper. The misfit dislocation lines and their Burgers vectors are parallel with the axis of the cylindrical inclusion (z-axis). For the material with a face-centered cubic (FCC) structure, the Burgers vectors are chosen as $\boldsymbol{b} = b/\sqrt{2}[1\ \bar{1}\ 0]$ and $\boldsymbol{b}' = -b/\sqrt{2}[1\ \bar{1}\ 0]$ for the nucleated dipole, where b is the magnitude of the Burgers vector.

Starting from a status where the investigated configuration is free of dislocations, the nucleation of misfit dislocation dipole will incur energy variation. If the total energy variation ΔW_{MSDD} due to the generation of the misfit dislocation dipole is negative, the nucleation process is energetically favorable and allowed, such criterion to be expressed as [16]

$$\Delta W_{\mathrm{MSDD}} = W_{\mathrm{d}} + W_{\mathrm{m}} \leq 0, \tag{1}$$

where W_{d} denotes the elastic energy of the MSDD per its unit length in the inclusion–matrix configuration, which is the energy barrier needed to be overcome for the nucleation; W_{m} is the energy arising from the elastic interaction between the MSDD and the misfit stress, which provides the driving force for the nucleation.

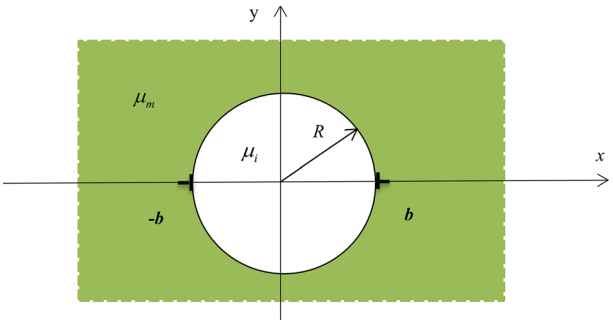

Fig. 1 MSDD at the interface between an inclusion and an infinite matrix

The final normalized nucleation energy for the MSDD is given as [13]

$$\Delta W^*_{\mathrm{MSDD}} = \frac{\Delta W_{\mathrm{MSDD}}}{\mu_{\mathrm{m}} b^2/2\pi} = \ln\frac{2R+r_0}{r_0} + \frac{\alpha-1}{\alpha+1}\ln\frac{R\,(R+r_0)+R^2}{R\,(R+r_0)-R^2} - \frac{8\pi a\varepsilon_{\mathrm{m}}R^2}{b\,(a+1)}\frac{1}{R+r_0}, \tag{2}$$

where r_0 is the dislocation core radius, ε_{m} is the misfit strain which was treated as eigenstrain (uniform shear strain) in evaluating W_{m} [43], and $\alpha = \mu_i/\mu_{\mathrm{m}}$ characterizes the relative shear modulus of the inclusion and the matrix.

3 Nucleation of a MEDD

According to the Frank's energy criterion [34], a full dislocation often dissociates into two partial dislocations connected through an SF ribbon if such dissociation is a process of energy decrease. Analyzing through the construction of the Thompson tetrahedron [34], the full screw dislocation dipole discussed above with Burgers vectors of $\boldsymbol{b}$ and $\boldsymbol{b}'$ is further split as

$$\begin{aligned} &\boldsymbol{b} \to \boldsymbol{b}_1 + \boldsymbol{b}_2, \\ &\frac{b}{\sqrt{2}}[1\ \bar{1}\ 0] \to \frac{\sqrt{2}b}{6}[2\ \bar{1}\ 1] + \frac{\sqrt{2}b}{6}[1\ \bar{2}\ \bar{1}], \end{aligned} \tag{3}$$

with $\boldsymbol{b}_1$ as the leading partial dislocation and $\boldsymbol{b}_2$ as the trailing partial dislocation and

$$\begin{aligned} &\boldsymbol{b}' \to \boldsymbol{b}_3 + \boldsymbol{b}_4, \\ &-\frac{b}{\sqrt{2}}[1\ \bar{1}\ 0] \to -\frac{\sqrt{2}b}{6}[1\ \bar{2}\ \bar{1}] - \frac{\sqrt{2}b}{6}[2\ \bar{1}\ 1], \end{aligned} \tag{4}$$

with $\boldsymbol{b}_3$ as the trailing partial dislocation and $\boldsymbol{b}_4$ as the leading partial dislocation. As mentioned in part 2, for strong nonlinear coupling among the parameters to be studied in the following, the analyzed MEDD configuration containing the four partials above is simplified with its trialling partials at the interface and leading partials in the matrix for a buried strained nanoscale inclusion within the matrix, as schematically shown in Fig. 2, and the two partials are connected through an SF ribbon with a width of p. Specifically, the leading partial dislocation $\boldsymbol{b}_1$ and trailing partial dislocation $\boldsymbol{b}_2$ are located at $x_1 = R + p$ and $x_2 = R$, while the symmetrical distribution of trailing partial dislocation $\boldsymbol{b}_3$ and leading partial dislocation $\boldsymbol{b}_4$ are located at $x_3 = -R$, $x_4 = -(R + p)$, respectively.

A more specific illustration of the decomposition of the full screw dislocation located at the phase interface $x = R$ is given in Fig. 3a, while the full screw dislocation located at the phase interface $x = -R$ decomposes in a similar and symmetrical process. The dissociated partial dislocations are all mixed dislocations with the line directions and Burgers vectors neither perpendicular nor parallel, i.e., they consist of both screw and edge characters. Since the problem regarding mixed partial dislocations can be solved as a superposition of plane strain problem for edge character and anti-plane strain problem for screw character, the partial dislocations are further decomposed into edge and screw parts along the $x([1\ 1\ 2])$ and $z([1\ \bar{1}\ 0])$ axes, respectively, as shown in Fig. 3b. In the configuration considered here, the Burgers vector components of the four partial

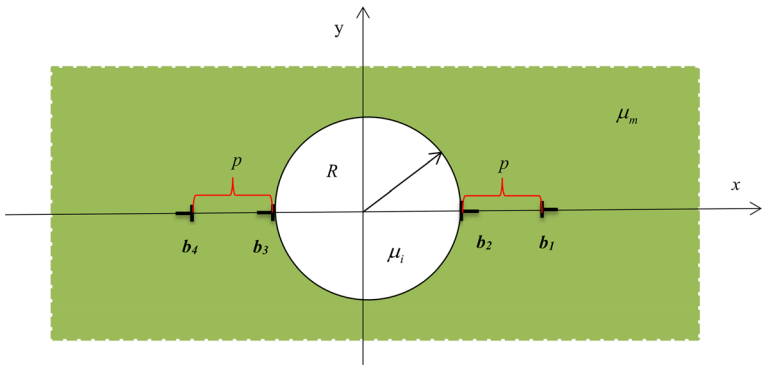

Fig. 2 MEDD near the inclusion within an infinite matrix

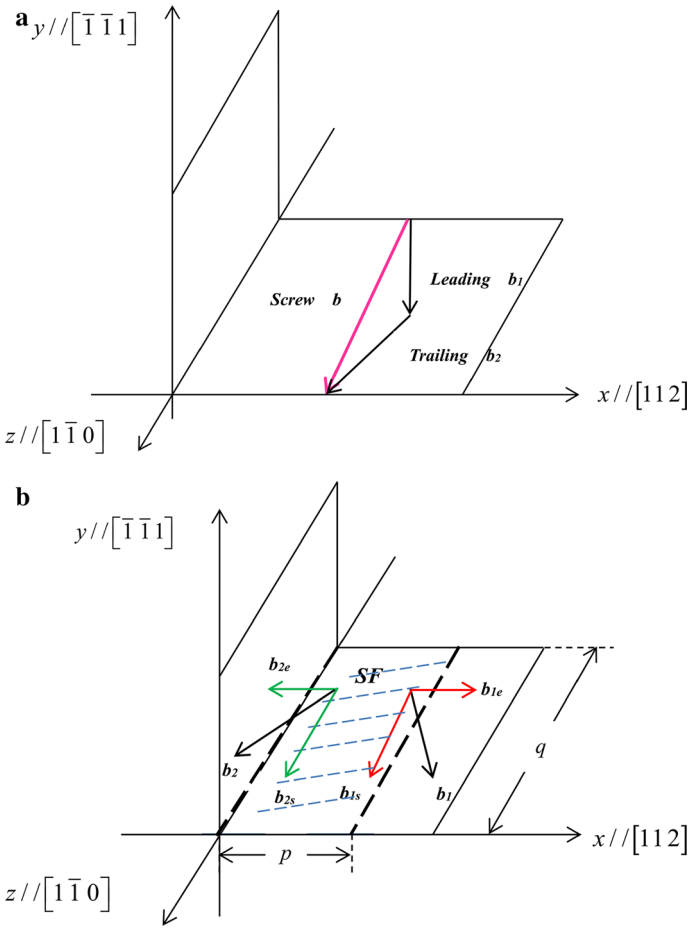

Fig. 3 **a** The decomposition of a screw dislocation into two partials, **b** the partials decomposed again into screw and edge parts

dislocations meet the relationships that $\boldsymbol{b}_{1e} = -\boldsymbol{b}_{2e} = \boldsymbol{b}_{3e} = -\boldsymbol{b}_{4e}$ and $\boldsymbol{b}_{1s} = \boldsymbol{b}_{2s} = -\boldsymbol{b}_{3s} = -\boldsymbol{b}_{4s}$, where $\boldsymbol{b}_{ne}$ $(n = 1,\ 2,\ 3,\ 4)$ are the edge components and $\boldsymbol{b}_{ns}$ $(n = 1, 2, 3, 4)$ are the screw components.

Different from the criterion for the formation of an MSDD, the criterion for the nucleation of an MEDD is

$$\Delta W_{\mathrm{MEDD}} = W_{\mathrm{d}} + W_{\mathrm{m}} + W_{\mathrm{s}} \leq 0, \tag{5}$$

where ΔW_{MEDD} denotes the total energy variation due to the nucleation of the MEDD, which consists of three contributions, i.e., W_{d} representing the elastic energy of the MEDD per its unit length, W_{m} representing the elastic energy due to the interaction between the misfit stress and the MEDD, and the SF energy W_{s}. For an

MEDD to be nucleated, the driving energy coming from W_{m} should overcome the energy barriers coming from W_{d} and W_{s}.

It is noted that there is no interaction energy between the screw and edge dislocations since their dislocation lines are parallel to each other; thus, the elastic energy of a mixed dislocation can be treated as a simple summation of the screw and edge parts. Specifically, W_{d} is further divided into the edge part W_{de} and screw part W_{ds}, i.e.,

$$W_{\mathrm{d}} = W_{\mathrm{de}} + W_{\mathrm{ds}}. \tag{6}$$

In the configuration of MEDD, W_{de} is expressed as [34],

$$\begin{aligned} W_{\mathrm{de}} = {} & \frac{b_{1\mathrm{e}}}{2}\int_{x_1+r_0}^{N}\sigma_{xy}(x,0)\,\mathrm{d}x - \frac{b_{2\mathrm{e}}}{2}\int_{x_2+r_0}^{N}\sigma_{xy}(x,0)\,\mathrm{d}x \\ & + \frac{b_{3\mathrm{e}}}{2}\int_{x_3-r_0}^{-N}\sigma_{xy}(x,0)\,\mathrm{d}x - \frac{b_{4\mathrm{e}}}{2}\int_{x_4-r_0}^{-N}\sigma_{xy}(x,0)\,\mathrm{d}x, \end{aligned} \tag{7}$$

where N characterizes the material size and is taken to be $N \to \infty$ to represent the infinite matrix, and $b_{ne} = b\cos 60^\circ/\sqrt{3}$ is the magnitude of $\boldsymbol{b_{ne}}$ $(n = 1,\ 2,\ 3,\ 4)$. The stress component $\sigma_{xy}(x,0) = \sum_{n=1}^{4}\sigma_{xyn}(x,0)$ comprises the contributions from the edge part of the four partial dislocations, which is calculated as [44,45]

$$\sigma_{xyn}(x,0) = \frac{\mu_{\mathrm{m}} b\,(-1)^{n+1}}{2\sqrt{3}\pi\,(\kappa_{\mathrm{m}}+1)} \left\{ \begin{array}{l} 2\frac{1}{x-x_n} - (A+B)\frac{x_n}{xx_n-R^2} \\ -2A\frac{\beta_n^2-1}{\beta_n^3}\left(1-\frac{\beta_n^2-1}{\beta_n}\frac{R}{x-\frac{R^2}{x_n}}\right)\frac{R}{\left(x-\frac{R^2}{x_n}\right)^2} \\ +(B-A)\frac{1}{\beta_n}\frac{R}{x^2} + (A+B)\frac{1}{x} - 2A\frac{R^2}{x^3} \end{array} \right\}, \tag{8}$$

where $A = (1-\alpha)/(1+\alpha\kappa_{\mathrm{m}})$, $B = (\kappa_i - \alpha\kappa_{\mathrm{m}})/(\kappa_i+\alpha)$, $\beta_n = x_n/R$ $(n = 1,\ 2,\ 3,\ 4)$, and κ is taken to be $3-4\nu$ for plane strain. The elastic energy of the screw components can be expressed as

$$\begin{aligned} W_{\mathrm{ds}} = {} & \frac{b_{1\mathrm{s}}}{2}\int_{x_1+r_0}^{N}\sigma_{yz}\,\mathrm{d}x + \frac{b_{2\mathrm{s}}}{2}\int_{x_2+r_0}^{N}\sigma_{yz}\,\mathrm{d}x \\ & - \frac{b_{3\mathrm{s}}}{2}\int_{x_3-r_0}^{-N}\sigma_{yz}\,\mathrm{d}x - \frac{b_{4\mathrm{s}}}{2}\int_{x_4-r_0}^{-N}\sigma_{yz}\,\mathrm{d}x, \end{aligned} \tag{9}$$

where $b_{ns} = b\cos 30^\circ/\sqrt{3}$ is the magnitude of $\boldsymbol{b_{ns}}$ $(n = 1,\ 2,\ 3,\ 4)$, and the stress component $\sigma_{yz}(x,0) = \sum_{n=1}^{4}\sigma_{yzn}(x,0)$ comprises the contributions from the screw part of the four partial dislocations, which is calculated as [46]

$$\sigma_{yzn}(x,0) = \lambda\left(\frac{\mu_{\mathrm{m}} b}{4\pi}\frac{1}{x-x_n} + \frac{k\mu_{\mathrm{m}} bR^2}{4\pi}\frac{1}{x(x_n x - R^2)}\right), \tag{10}$$

with $\lambda = 1$ for $n = 1,\ 2$ and $\lambda = -1$ for $n = 3,\ 4$.

The elastic energy due to the interaction between the misfit stress and the MEDD can also be divided into the edge part W_{me} and screw part W_{ms}

$$W_{\mathrm{m}} = W_{\mathrm{me}} + W_{\mathrm{ms}}. \tag{11}$$

For the edge part,

$$\begin{aligned} W_{\mathrm{me}} = {} & -b_{1\mathrm{e}}\int_{x_1+r_0}^{N}\sigma_{xym}(x,0)\,\mathrm{d}x + b_{2\mathrm{e}}\int_{x_2+r_0}^{N}\sigma_{xym}(x,0)\,\mathrm{d}x \\ & - b_{3\mathrm{e}}\int_{x_3-r_0}^{-N}\sigma_{xym}(x,0)\,\mathrm{d}x + b_{4\mathrm{e}}\int_{x_4-r_0}^{-N}\sigma_{xym}(x,0)\,\mathrm{d}x, \end{aligned} \tag{12}$$

which is omitted since the misfit stress component $\sigma_{xym}(x,0)$ is equal to zero for the current plane problem of a buried strained cylindrical inclusion within the infinite matrix [14,16], while for the screw part,

$$W_{\mathrm{ms}} = -b_{1\mathrm{s}}\int_{x_1+r_0}^{N}\sigma_{yzm}(x,0)\,\mathrm{d}x - b_{2\mathrm{s}}\int_{x_2+r_0}^{N}\sigma_{yzm}(x,0)\,\mathrm{d}x$$

$$+b_{3\mathrm{s}}\int_{x_3-r_0}^{-N}\sigma_{yzm}(x,0)\,\mathrm{d}x\;+b_{4\mathrm{s}}\int_{x_4-r_0}^{-N}\sigma_{yzm}(x,0)\,\mathrm{d}x, \tag{13}$$

the misfit stress $\sigma_{yzm}(x,0)$ is calculated from the complex potential method as [13]

$$\sigma_{yzm}(x,0)=\frac{2\mu_i\mu_{\mathrm{m}}\varepsilon_{\mathrm{m}}}{\mu_i+\mu_{\mathrm{m}}}\frac{R^2}{x^2}. \tag{14}$$

The energy of the SF ribbon is

$$W_{\mathrm{s}}=\gamma s=\gamma p, \tag{15}$$

where γ is the intrinsic SF energy per unit area and s is the area of the SF ribbon and equal to the ribbon width for the considered dislocation lines of unit length.

Combining the three parts of energy contribution calculated from Eqs. (6), (11) and (15) into the nucleation energy ΔW_{MEDD} of the MEDD shown in Eq. (5), and normalizing the nucleation energy ΔW_{MEDD} by $\mu_{\mathrm{m}}b^2/2\pi$ similar to the normalized treatment in Eq. (2), the nucleation criterion for the MEDD is finally given as

$$\begin{aligned}\Delta W'_{\mathrm{MEDD}}&=\frac{\Delta W_{\mathrm{MEDD}}}{\mu_{\mathrm{m}}b^2/2\pi}\\&=\sum_{n=1}^{4}\frac{(-1)^n}{12\pi\,(\kappa_{\mathrm{m}}+1)}\left\{\begin{array}{l}2\ln\frac{(x_n+r_0-x_1)(x_n+r_0-x_3)}{(x_n+r_0-x_2)(x_n+r_0-x_4)}\\-(A+B)\ln\frac{\left(x_1(x_n+r_0)-R^2\right)\left(x_3(x_n+r_0)-R^2\right)}{\left(x_2(x_n+r_0)-R^2\right)\left(x_4(x_n+r_0)-R^2\right)}\\+2AR\sum\limits_{j=1}^{4}\frac{\beta_j^2-1}{(-1)^j\beta_j^3}\frac{x_j}{x_j(x_n+r_0)-R^2}\\-AR^2\sum\limits_{j=1}^{4}\frac{\left(\beta_j^2-1\right)^2}{(-1)^j\beta_j^4}\frac{x_j^2}{\left(x_j(x_n+r_0)-R^2\right)^2}\\-(B-A)\left(\frac{1}{\beta_1}-\frac{1}{\beta_2}+\frac{1}{\beta_3}-\frac{1}{\beta_4}\right)\frac{R}{x_n+r_0}\end{array}\right\}\\&\quad-\frac{k}{4}\ln\frac{\left(R^2-(x_2+r_0)\,x_1\right)\left(R^2-(x_2+r_0)\,x_2\right)}{\left(R^2-(x_2+r_0)\,x_3\right)\left(R^2-(x_2+r_0)\,x_4\right)}\\&\quad+\frac{1}{8}\ln\frac{(x_2+r_0-x_1)\,(x_2+r_0-x_2)}{(x_2+r_0-x_3)\,(x_2+r_0-x_4)}\frac{(x_3-r_0-x_1)\,(x_3-r_0-x_2)}{(x_3-r_0-x_3)\,(x_3-r_0-x_4)}\end{aligned}$$

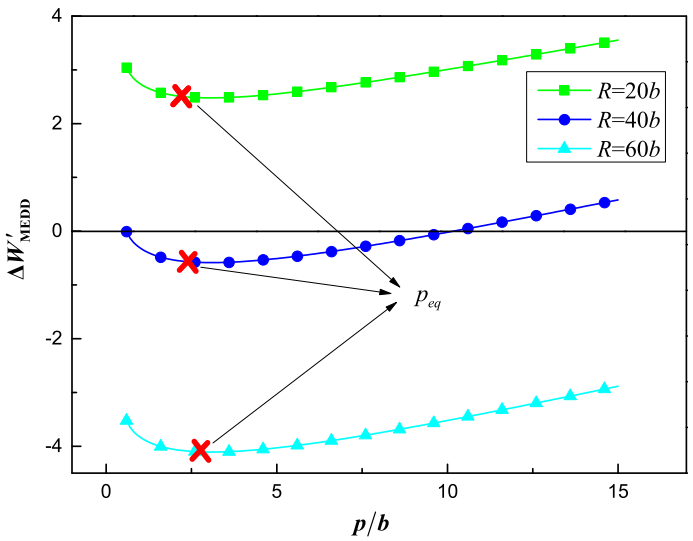

Fig. 4 Nucleation energy for MEDD $\Delta W'_{\mathrm{MEDD}}$ as a function of the separation p with various inclusion radius R for $\alpha=5$, $\gamma^*=0.1$, $\varepsilon_m=0.005$, $\nu_i=\nu_m=0.3$ and $r_0=0.5b$

$$
\begin{aligned}
&-\frac{1}{4}\ln\frac{(x_1+r_0-x_1)(x_1+r_0-x_2)}{(x_1+r_0-x_3)(x_1+r_0-x_4)}\\
&-\frac{k}{4}\ln\frac{\left(R^2-(x_1+r_0)x_1\right)\left(R^2-(x_1+r_0)x_2\right)}{\left(R^2-(x_1+r_0)x_3\right)\left(R^2-(x_1+r_0)x_4\right)}\\
&-\frac{2\pi\mu_i\varepsilon_{\mathrm{m}}R^2}{b(\mu_i+\mu_{\mathrm{m}})}\left(\frac{1}{x_1+r_0}+\frac{1}{x_2+r_0}-\frac{1}{x_3-r_0}-\frac{1}{x_4-r_0}\right)+\frac{\gamma^* p}{b}\\
&\le 0, \qquad (16)
\end{aligned}
$$

where $\gamma^* = \gamma/(\mu_{\mathrm{m}} b/2\pi)$ represents reduced SF energy.

For the energetically favorable nucleation of an MEDD, there is an equilibrium separation of the SF ribbon p_{eq}, which results in a minimum nucleation energy. The MEDD with SF ribbon of such width is most preferred to nucleate. Therefore, to obtain the equilibrium separation of the SF ribbon which minimizes the nucleation energy, the relationship between the nucleation energy $\Delta W'_{\mathrm{MEDD}}$ and the SF ribbon width p is plotted in Fig. 4 for $\nu_i = \nu_{\mathrm{m}} = 0.3$, $r_0 = 0.5b$, $\alpha = 5$, $\gamma^* = 0.1$, $\varepsilon_{\mathrm{m}} = 0.005$, and $R = 20b, 40b, 60b$, respectively.

It is shown in all the three lines that $\Delta W'_{\mathrm{MEDD}}$ decreases firstly and then increases with the increase of p, i.e., there is a saddle point when $p = p_{\mathrm{eq}}$, at which $\Delta W'_{\mathrm{MEDD}}$ approaches its minimum value. More studies

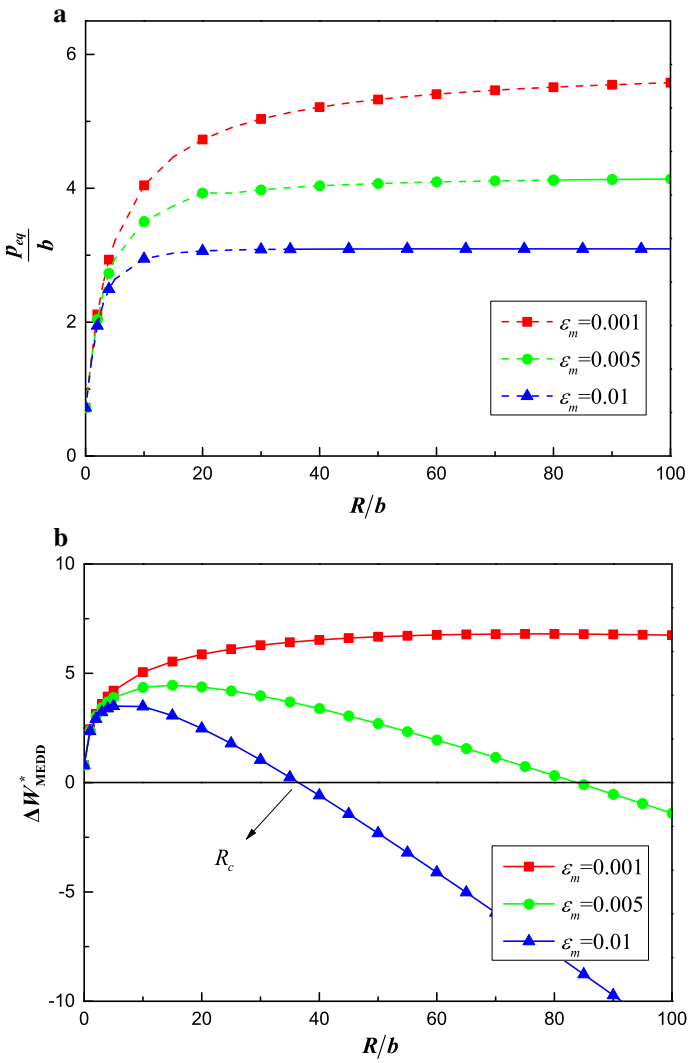

Fig. 5 **a** Equilibrium separation p_{eq}/b versus the radius of the inclusion R/b and **b** nucleation energy for MEDD $\Delta W^*_{\mathrm{MEDD}}$ versus the radius of the inclusion R/b, with various misfit strains ε_{m} for $\alpha = 5$, $\gamma^* = 0.1$, $\nu_i = \nu_{\mathrm{m}} = 0.3$ and $r_0 = 0.5b$

on the relationship between $\Delta W'_{\mathrm{MEDD}}$ and p with different parameter combinations also give similar curves as shown in Fig. 4; thus, no more tautology is here. Therefore, the equilibrium separation p_{eq} of the extended dislocations, reflecting the nucleation site of the leading partials, can be obtained by minimizing the nucleation energy $\Delta W'_{\mathrm{MEDD}}$ (which is also adopted in [42])

$$\frac{\partial \Delta W'_{\mathrm{MEDD}}}{\partial p} = 0. \tag{17}$$

Substituting p by p_{eq} in Eq. (17) gives the final form of the minimum energy for the MEDD to be nucleated, denoted by $\Delta W^*_{\mathrm{MEDD}}$. It should be noted that the MEDD with SF ribbon width of p_{eq} cannot always nucleate if the minimum energy $\Delta W^*_{\mathrm{MEDD}}$ is still positive, which means that the energy barrier for nucleation cannot be overcome. According to this rule, it is difficult for MEDD to nucleate spontaneously in nanocomposites with inclusion size of $20b$ and $\nu_i = \nu_{\mathrm{m}} = 0.3$, $r_0 = 0.5b$, $\alpha = 5$, $\gamma^* = 0.1$, $\varepsilon_{\mathrm{m}} = 0.005$, while the nucleation criterion is met for $R = 40b$ and $R = 60b$.

It is evident that both the equilibrium separation p_{eq} of the extended dislocations and the corresponding nucleation energy $\Delta W^*_{\mathrm{MEDD}}$ are related to the inclusion radius R, the misfit strain ε_{m}, the relative shear modulus of the inclusion to the matrix $\alpha = \mu_i/\mu_{\mathrm{m}}$ and the reduced SF energy per unit area γ^*. However, such relationship cannot be explicitly obtained due to the strong nonlinear coupling among the above-

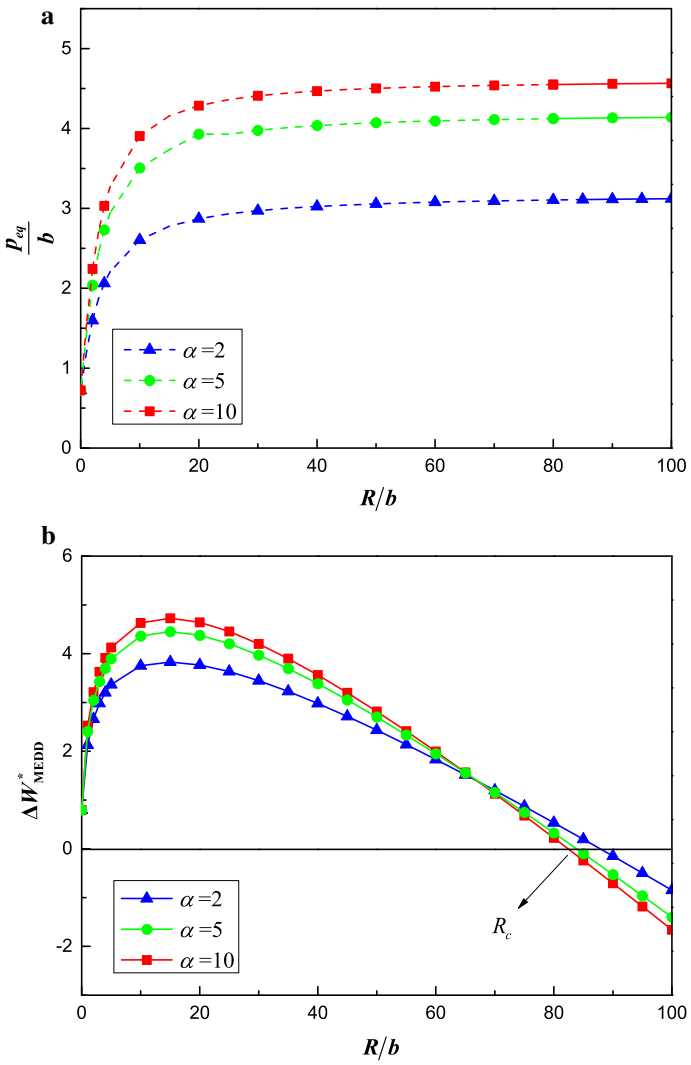

Fig. 6 **a** Equilibrium separation p_{eq}/b versus the radius of the inclusion R/b and **b** nucleation energy for MEDD $\Delta W^*_{\mathrm{MEDD}}$ versus the radius of the inclusion R/b, with various α for $\varepsilon_{\mathrm{m}} = 0.005$, $\gamma^* = 0.1$, $\nu_i = \nu_{\mathrm{m}} = 0.3$ and $r_0 = 0.5b$

mentioned factors. Thus, the effects of these factors on the nucleation of MEDD will be numerically investigated.

Figure 5a is plotted as the equilibrium separation p_{eq}/b versus the inclusion radius R/b and Fig. 5b is plotted as the nucleation energy $\Delta W^*_{\mathrm{MEDD}}$ versus the inclusion radius R/b with various ε_{m} both for $\alpha = 5$, $\gamma^* = 0.1$, $\nu_i = \nu_{\mathrm{m}} = 0.3$ and $r_0 = 0.5b$ to investigate the influence of the misfit strain. From Fig. 5a it is found that when other parameters are fixed, the equilibrium separation p_{eq} of the extended dislocations which minimizes the nucleation energy increases with the increase of the inclusion radius R/b. Furthermore, as R/b approaches about 30, p_{eq} tends to be saturated and will not increase any more with further increase of R/b. Figure 5a also shows that lower misfit strain will lead to wider equilibrium separation p_{eq}. However, from Fig. 5b we can see that the nucleation condition is satisfied only when the inclusion radius reaches a critical value R_{c}. If the inclusion size is smaller than R_{c}, the nucleation energy $\Delta W^*_{\mathrm{MEDD}}$ is positive, and the MEDD cannot nucleate spontaneously, which is consistent with the finding in Fig. 4. Thus, the equilibrium separation p_{eq} minimizing the nucleation energy is not always the real SF ribbon width of the nucleated MEDD; the parts of p_{eq} are shown in Fig. 5a with dot lines. Moreover, the higher ε_{m} is, the easier for the MEDD to be nucleated, as shown in Fig. 5b, indicating that the misfit strain should be high enough for the MEDD to be nucleated, which is in agreement with the earlier conclusion for a MSDD [13].

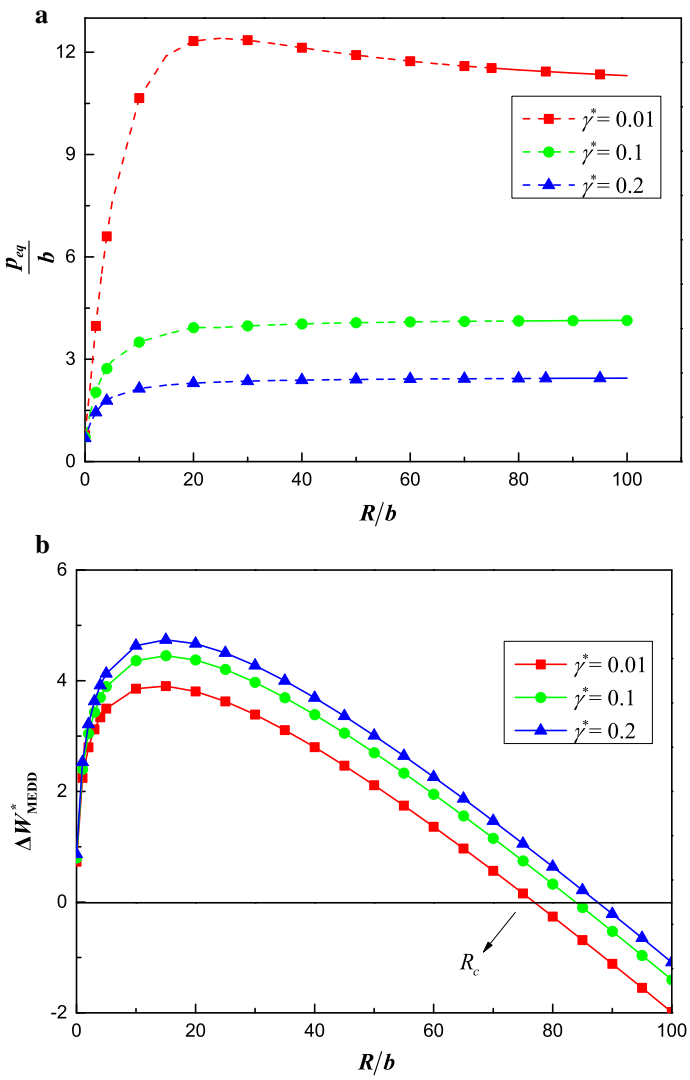

Fig. 7 **a** Equilibrium separation p_{eq}/b versus the radius of the inclusion R/b and **b** nucleation energy for MEDD $\Delta W^*_{\mathrm{MEDD}}$ versus the radius of the inclusion R/b, with various γ^* for $\varepsilon_{\mathrm{m}} = 0.005$, $\alpha = 5$, $\nu_i = \nu_{\mathrm{m}} = 0.3$ and $r_0 = 0.5b$

The influence of the relative shear modulus of the inclusion to the matrix $\alpha = \mu_i/\mu_\mathrm{m}$ on the nucleation of the MEDD is shown in Fig. 6. Figure 6a is plotted as $p_\mathrm{eq}/b - R/b$ and Fig. 6b is plotted as $\Delta W^*_\mathrm{MEDD} - R/b$ with various α for $\varepsilon_\mathrm{m} = 0.005$, $\gamma^* = 0.1$, $\nu_i = \nu_\mathrm{m} = 0.3$ and $r_0 = 0.5b$. Figure 6a shows a similar tendency as Fig. 5a, i.e., the equilibrium separation p_eq increases with the increase of R/b and will be saturated when $R/b \approx 30$; higher shear modulus ratio leads to wider p_eq. In Fig. 6b, it is shown that the critical inclusion radius R_c decreases with the increase of the ratio of the shear modulus $\alpha = \mu_i/\mu_\mathrm{m}$.

The relationships of $p_\mathrm{eq}/b - R/b$ and $\Delta W^*_\mathrm{MEDD} - R/b$ are plotted in Fig. 7a, b, respectively, with various γ^* for $\alpha = 5$, $\varepsilon_\mathrm{m} = 0.005$ and $\nu_i = \nu_\mathrm{m} = 0.3$. Figure 7a also shows the tendency that p_eq increases with the increase of R/b until it reaches a saturation value at $R/b \approx 30$, except for that of $\gamma^* = 0.01$, where a little decline occurs after p_eq reaching the maximum. There also are some p_eq that are spurious for the MEDD to be nucleated, shown as dot lines in Fig. 7a. Moreover, lower γ^* leads to wider p_eq, which is also in agreement with the earlier statement [39]. In Fig. 7b, the critical inclusion radius R_c increases with the increase of the reduced SF energy per unit area, indicating that it is easier for the material with lower SF energy to nucleate MEDD.

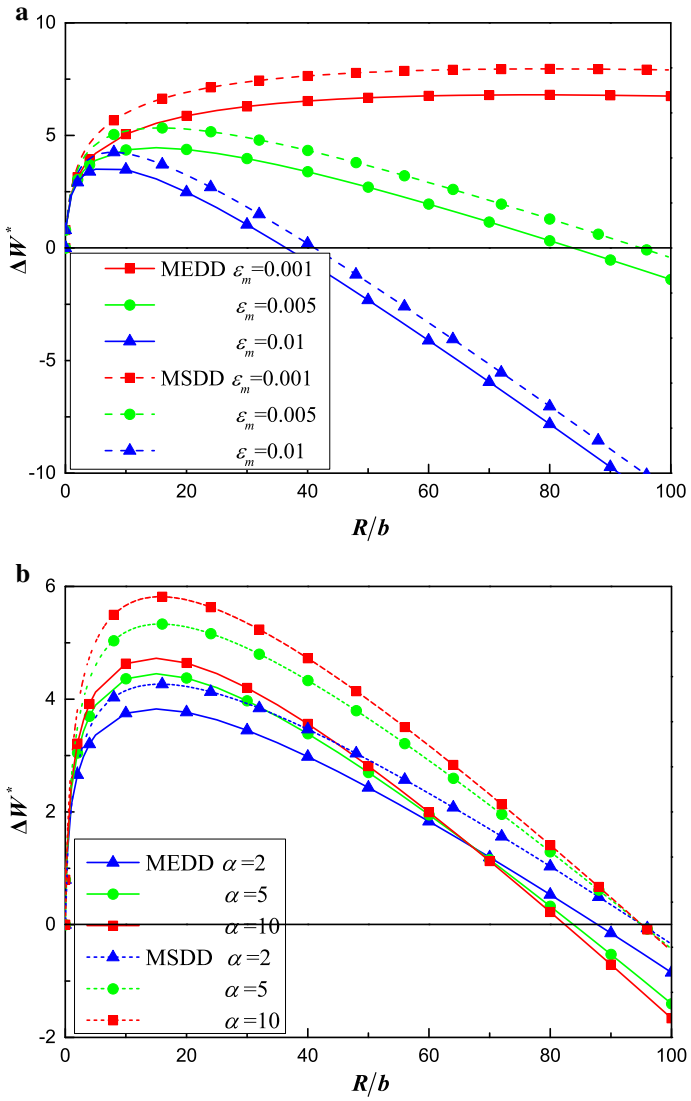

Fig. 8 **a** Nucleation energy for MEDD or MSDD ΔW^* versus the radius of the inclusion R/b with various ε_m for $\alpha = 5$, $\gamma^* = 0.1$, $\nu_i = \nu_\mathrm{m} = 0.3$, and $r_0 = 0.5b$; **b** nucleation energy for MEDD or MSDD ΔW^* versus the radius of the inclusion R/b with various α for $\varepsilon_\mathrm{m} = 0.005$, $\gamma^* = 0.1$, $\nu_i = \nu_\mathrm{m} = 0.3$ and $r_0 = 0.5b$

In conclusion, it is found that once the nucleation criterion for the MEDD is satisfied, lower misfit strain and intrinsic SF energy lead to wider p_{eq}, while higher shear modulus ratio leads to wider p_{eq}. Inspired by these findings, the preferred nucleation of a wider SF width, which may eventually trigger the form of embryonic twins serving as the potential strengthening mechanism for nanocomposites, can be achieved through increasing the inclusion radius and shear modulus ratio while lowering the SF energy and misfit strain.

4 The competitive nucleation between the MEDD and MSDD

In former sections, we have discussed the nucleation of two different defect configurations—MSDD and MEDD in nanocomposites. It is noted that these two different kinds of defects could lead to contrary material properties; therefore, it is necessary to investigate the competition between these two nucleation possibilities.

Misfit strain and modulus difference are the sources of the nucleation of the defects at the interface of nanocomposites. Figure 8a, b is plotted as the nucleation energy of both the MEDD and MSDD versus the inclusion radius R/b with various misfit strain ε_m and shear modulus ratio α, respectively, to investigate the influence of these two parameters on the competitive nucleation relationship. Both of the two plots show that with the parameters selected, the MEDD is easier to nucleate than the MSDD. It is noted that the nucleation energy for MEDD ΔW^*_{MEDD} increases with the further increase of SF energy γ^*. Thus, the MSDD could be easier to nucleate than MEDD if γ^* is larger than the specified value of $\gamma^* = 0.1$. This indicates that there is a critical reduced SF energy γ^*_c at which the preferred nucleation mechanism will transfer from MEDD to MSDD. It is suspected that γ^*_c could be affected by the misfit strain ε_m, shear modulus ratio α and inclusion radius R; such influences will be systematically investigated in the following.

Misfit strain ε_m is the dominant source for the nucleation of defects, and its effect on the transition of nucleation is investigated through the plot in Fig. 9, where the relationship between ΔW^* and γ^* is shown with three different misfit strains $\varepsilon_m = 0.005$, 0.0075 and 0.01, while other parameters are taken as $\alpha = 5$, $R = 100b$, $\nu_i = \nu_m = 0.3$ and $r_0 = 0.5b$. It is found that the nucleation energy for MEDD ΔW^*_{MEDD} increases nonlinearly with the increase of γ^* due to the influence of γ^* on the equilibrium ribbon width p_{eq}, which also affects the nucleation energy. Moreover, ΔW^*_{MEDD} has an intersection with the nucleation energy of the MSDD ΔW^*_D at a critical value γ^*_c. Beyond this value, $\Delta W^*_{\text{MEDD}} \geq \Delta W^*_{\text{MSDD}}$; thus, the MSDD is preferred to nucleate, while the MEDD is easier to nucleate when $\gamma^* < \gamma^*_c$. It is also found that γ^*_c decreases slightly with the increase of the misfit strain ε_m, indicating that lower ε_m will stimulate the nucleation transferring from MSDD to MEDD for the matrix with specific stack fault energy ($\gamma^* \approx 0.6$ for the investigated case here).

The influence of the shear modulus ratio α is shown in Fig. 10 as $\Delta W^* - \gamma^*$ with three different shear modulus ratios $\alpha = 5$, 7.5 and 10 for $\varepsilon_m = 0.005$, $R = 100b$, $\nu_i = \nu_m = 0.3$ and $r_0 = 0.5b$. The effect of

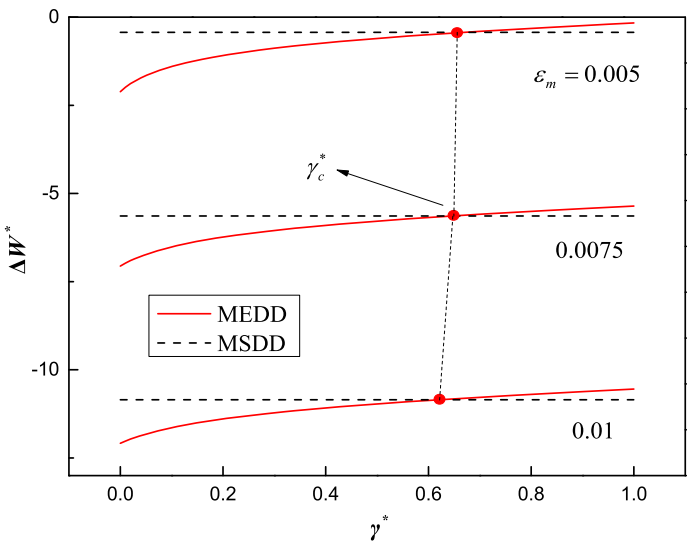

Fig. 9 Nucleation energy for MEDD or MSDD ΔW^* versus the stacking fault energy γ^* with various ε_m for $\alpha = 5$, $R = 100b$, $\nu_i = \nu_m = 0.3$ and $r_0 = 0.5b$

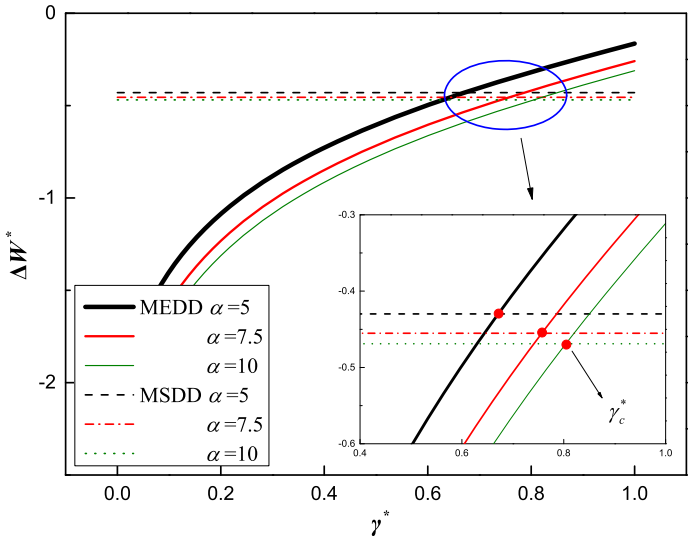

Fig. 10 Nucleation energy for MEDD or MSDD ΔW^* versus the stacking fault energy γ^* with various α for $\varepsilon_m = 0.005$, $R = 100b$, $\nu_i = \nu_m = 0.3$ and $r_0 = 0.5b$

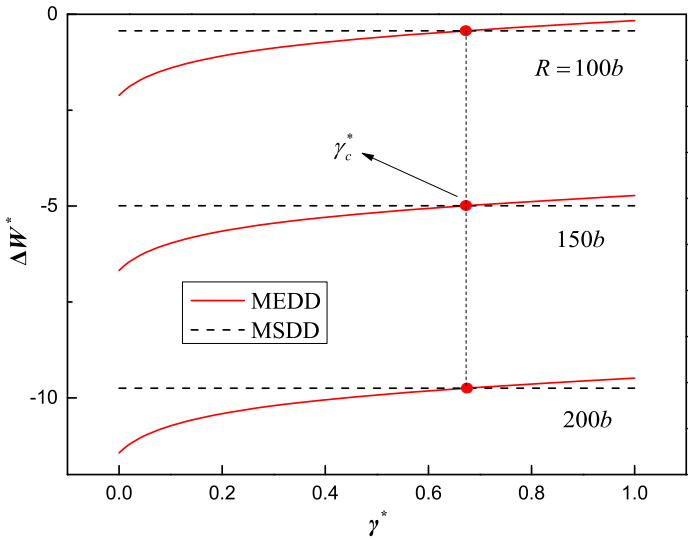

Fig. 11 Nucleation energy for MEDD or MSDD ΔW^* versus the stacking fault energy γ^* with various R for $\varepsilon_m = 0.005$, $\alpha = 5$, $\nu_i = \nu_m = 0.3$ and $r_0 = 0.5b$

γ^* is similar to the results shown in Fig. 9. Moreover, γ_c^* decreases slightly with the decrease of α, indicating that larger shear modulus ratio is preferred for nucleation transformation from MSDD to MEDD for matrix with specific stack fault energy ($\gamma^* \approx 0.7$ for the investigated case here).

The variation in the nucleation energy versus the reduced SF energy is depicted in Fig. 11 at different values of inclusion radius $R = 100b$, $150b$ and $200b$ for $\varepsilon_m = 0.005$, $\alpha = 5$, $\nu_i = \nu_m = 0.3$ and $r_0 = 0.5b$. Similar intersection between the nucleation energy of the MEDD and MSDD is presented as shown in Figs. 9 and 10. The result also indicates that the critical value γ_c^* for the transition between MEDD and MSDD is almost not affected by R.

Therefore, conclusion can be given from Figs. 9, 10 and 11 that the reduced SF energy γ^* determines the preferred nucleation between MSDD and MEDD, and the MEDD can nucleate more easily in the materials with lower intrinsic SF energy; the misfit strain ε_m and the shear modulus ratio α will affect the competitive nucleation between MEDD and MSDD for the matrix with specific stack fault energy, while inclusion radius R has negligible effect on the competitive nucleation.

5 Conclusion

Similar to the nucleation of MSDD at the interface of nanocomposites, the nucleation of MEDD is energetically favorable when the inclusion radius approaches a critical value. The critical radius for the nucleation of MEDD decreases with the increase of misfit strain and shear modulus ratio, while with the decreased SF energy. Furthermore, the equilibrium SF width of the nucleated MEDD increases with the increase of radius of inclusion and is wider for nanocomposites with lower misfit strain, higher shear modulus ratio and lower SF energy. The intrinsic SF energy is the dominant factor affecting the competitive nucleation between MEDD and MSDD, and MEDD is more preferable to nucleate for the matrix with lower SF energy. The critical SF energy for the nucleation transferring from MSDD to MEDD increases with the increase of the shear modulus ratio and decrease of the misfit strain, while it is almost not affected by the inclusion radius. Nevertheless, as mentioned above, the surface/interface effect and preferred dislocation location should also be considered for approximating the real situation. Further research will take this into account and focus on the comparison of the analysis displayed in this paper with some novel experiments. Moreover, other dislocation configurations such as edge dislocation will also be studied in the future to systematize this work.

Acknowledgements The authors would like to appreciate the support of NSFC (11202172), the Basic Application Research Plan of Sichuan Province (2015JY0239) and the Sichuan Provincial Youth Science and Technology Innovation Team (2013TD0004). The research is also supported by the Opening fund of State Key Laboratory of Nonlinear Mechanics.

References

1. Karnesky, R.A., Meng, L., Dunand, D.C.: Strengthening mechanisms in aluminum containing coherent Al_3Sc precipitates and incoherent Al_2O_3 dispersoids. Acta Mater. **55**(4), 1299–1308 (2007)
2. Chen, J., Costan, E., Van Huis, M., Xu, Q., Zandbergen, H.: Atomic pillar-based nanoprecipitates strengthen AlMgSi alloys. Science **312**(5772), 416–419 (2006)
3. Van der Merwe, J.H.: Misfit dislocation generation in epitaxial layers. Crit. Rev. Solid State Mater. Sci. **17**(3), 187–209 (1991)
4. Jain, S., Harker, A., Cowley, R.: Misfit strain and misfit dislocations in lattice mismatched epitaxial layers and other systems. Philos. Mag. A **75**(6), 1461–1515 (1997)
5. Ovid'ko, I.A.: Relaxation mechanisms in strained nanoislands. Phys. Rev. Lett. **88**(4), 046103 (2002)
6. Freund, L.B., Suresh, S.: Thin Film Materials: Stress, Defect Formation and Surface Evolution. Cambridge University Press, Cambridge (2004)
7. Ovid ko, I., Sheinerman, A.: Nanoparticles as dislocation sources in nanocomposites. J. Phys. Condens. Matter **18**(19), L225 (2006)
8. Aifantis, K.E., Kolesnikova, A.L., Romanov, A.E.: Nucleation of misfit dislocations and plastic deformation in core/shell nanowires. Philos. Mag. **87**(30), 4731–4757 (2007). doi:10.1080/14786430701589350
9. Appel, F., Fischer, F., Clemens, H.: Precipitation twinning. Acta Mater. **55**(14), 4915–4923 (2007)
10. Freund, L., Gosling, T.: Critical thickness condition for growth of strained quantum wires in substrate V-grooves. Appl. Phys. Lett. **66**(21), 2822–2824 (1995)
11. Gosling, T.J., Freund, L.B.: A critical thickness condition for triangular strained quantum wires grown in V-grooves on a patterned substrate. Acta Mater. **44**(1), 1–13 (1996). doi:10.1016/1359-6454(95)00173-X
12. Colin, J., Grilhé, J.: Surface instability and delamination of epitaxially stressed bilayers. Philos. Mag. A Phys. Condens. Matter Struct. Defects Mech. Prop. **82**(13), 2609–2621 (2002). doi:10.1080/01418610210152800
13. Fang, Q., Liu, Y., Chen, J.: Misfit dislocation dipoles and critical parameters of buried strained nanoscale inhomogeneity. Appl. Phys. Lett. **92**(12), 121923 (2008)
14. Fang, Q., Liu, Y., Wen, P.: Dipole of edge misfit dislocations and critical radius conditions for buried strained cylindrical inhomogeneity. Philos. Mag. **89**(20), 1585–1595 (2009)
15. Kolesnikova, A.L., Romanov, A.E.: Misfit dislocation loops and critical parameters of quantum dots and wires. Philos. Mag. Lett. **84**(8), 501–506 (2004). doi:10.1080/09500830412331305274
16. Gutkin, M.Y., Ovid'ko, I., Sheinerman, A.: Misfit dislocations in wire composite solids. J. Phys. Condens. Matter **12**(25), 5391 (2000)
17. Duan, H.L., Wang, J., Huang, Z.P., Karihaloo, B.L.: Size-dependent effective elastic constants of solids containing nano-inhomogeneities with interface stress. J. Mech. Phys. Solids **53**(7), 1574–1596 (2005). doi:10.1016/j.jmps.2005.02.009
18. Quang, H.L., He, Q.C.: Size-dependent effective thermoelastic properties of nanocomposites with spherically anisotropic phases. J. Mech. Phys. Solids **55**(9), 1899–1931 (2007). doi:10.1016/j.jmps.2007.02.005
19. Mogilevskaya, S.G., Crouch, S.L., Stolarski, H.K., Benusiglio, A.: Equivalent inhomogeneity method for evaluating the effective elastic properties of unidirectional multi-phase composites with surface/interface effects. Int. J. Solids Struct. **47**(3–4), 407–418 (2010). doi:10.1016/j.ijsolstr.2009.10.007
20. Zhao, Y., Fang, Q., Liu, Y.: Edge misfit dislocations in core–shell nanowire with surface/interface effects and different elastic constants. Int. J. Mech. Sci. **74**, 173–184 (2013)
21. Fan, H., Wang, G.F.: Screw dislocation interacting with imperfect interface. Mech. Mater. **35**(10), 943–953 (2003). doi:10.1016/S01676636(02)00309-5

22. Wang, X.: Interaction between an edge dislocation and a circular inclusion with an inhomogeneously imperfect interface. Mech. Res. Commun. **33**(1), 17–25 (2006). doi:10.1016/j.mechrescom.2005.05.002
23. Wang, X., Pan, E., Roy, A.K.: New phenomena concerning a screw dislocation interacting with two imperfect interfaces. J. Mech. Phys. Solids **55**(12), 2717–2734 (2007). doi:10.1016/j.jmps.2007.03.017
24. Fang, Q.H., Jin, B., Liu, Y., Liu, Y.W.: Interaction between screw dislocations and inclusions with imperfect interfaces in fiber-reinforced composites. Acta Mech. **203**(1), 113–125 (2009). doi:10.1007/s00707-008-0038-2
25. Sudak, L.J.: On the interaction between a dislocation and a circular inhomogeneity with imperfect interface in antiplane shear. Mech. Res. Commun. **30**(1), 53–59 (2003). doi:10.1016/S0093-6413(02)00352-X
26. Wang, X., Schiavone, P.: Interaction between an edge dislocation and a circular inhomogeneity with a mixed-type imperfect interface. Arch. Appl. Mech. (2016). doi:10.1007/s00419-016-1178-9
27. Fang, Q.H., Liu, Y.W.: Size-dependent elastic interaction of a screw dislocation with a circular nano-inhomogeneity incorporating interface stress. Scr. Mater. **55**(1), 99–102 (2006). doi:10.1016/j.scriptamat.2006.03.026
28. Fang, Q.H., Liu, Y.W.: Size-dependent interaction between an edge dislocation and a nanoscale inhomogeneity with interface effects. Acta Mater. **54**(16), 4213–4220 (2006). doi:10.1016/j.actamat.2006.05.012
29. Liu, Y.W., Fang, Q.H.: Analysis of a screw dislocation inside an inhomogeneity with interface stress. Mater. Sci. Eng. A **464**(1–2), 117–123 (2007). doi:10.1016/j.msea.2007.02.057
30. Fang, Q.H., Liu, Y.W., Jin, B., Wen, P.H.: Interaction between a dislocation and a core–shell nanowire with interface effects. Int. J. Solids Struct. **46**(6), 1539–1546 (2009). doi:10.1016/j.ijsolstr.2008.11.026
31. Luo, J., Xiao, Z.M.: Analysis of a screw dislocation interacting with an elliptical nano inhomogeneity. Int. J. Eng. Sci. **47**(9), 883–893 (2009). doi:10.1016/j.ijengsci.2009.05.007
32. Shodja, H.M., Ahmadzadeh-Bakhshayesh, H., Gutkin, M.Y.: Size-dependent interaction of an edge dislocation with an elliptical nano-inhomogeneity incorporating interface effects. Int. J. Solids Struct. **49**(5), 759–770 (2012). doi:10.1016/j.ijsolstr.2011.11.013
33. Wang, X., Schiavone, P.: Interaction of a screw dislocation with a nano-sized, arbitrarily shaped inhomogeneity with interface stresses under anti-plane deformations. Proc. R. Soc. A Math. Phys. Eng. Sci. **470**(2170), 20140313 (2014)
34. Hirth, J.P., Lothe, J.: Theory of Dislocations, second edn. Wiley, New York (1982)
35. Lu, K., Lu, L., Suresh, S.: Strengthening materials by engineering coherent internal boundaries at the nanoscale. Science **324**(5925), 349–352 (2009). doi:10.1126/science.1159610
36. Lu, L., Lu, K.: Metallic materials with nano-scale twins. Jinshu Xuebao/Acta Metall. Sin. **46**(11), 1422–1427 (2010). doi:10.3724/sp.j.1037.2010.00462
37. Lu, L., Chen, X., Huang, X., Lu, K.: Revealing the maximum strength in nanotwinned copper. Science **323**(5914), 607–610 (2009). doi:10.1126/science.1167641
38. Zhang, X., Romanov, A., Aifantis, E.C.: A simple physically based phenomenological model for the strengthening/softening behavior of nanotwinned copper. J. Appl. Mech. **82**(12), 121005 (2015)
39. Roters, F., Eisenlohr, P., Hantcherli, L., Tjahjanto, D.D., Bieler, T.R., Raabe, D.: Overview of constitutive laws, kinematics, homogenization and multiscale methods in crystal plasticity finite-element modeling: theory, experiments, applications. Acta Mater. **58**(4), 1152–1211 (2010). doi:10.1016/j.actamat.2009.10.058
40. Zou, J., Cockayne, D.: Theoretical consideration of misfit dislocation nucleation by partial dislocations in [001] strained-layer heterostructures. J. Appl. Phys. **74**(2), 925–930 (1993)
41. Chen, M., Ma, E., Hemker, K.J., Sheng, H., Wang, Y., Cheng, X.: Deformation twinning in nanocrystalline aluminum. Science **300**(5623), 1275–1277 (2003). doi:10.1126/science.1083727
42. Asaro, R.J., Krysl, P., Kad, B.: Deformation mechanism transitions in nanoscale fcc metals. Philos. Mag. Lett. **83**(12), 733–743 (2003)
43. Rockenberger, J., Tröger, L., Rogach, A.L., Tischer, M., Grundmann, M., Eychmüller, A., Weller, H.: The contribution of particle core and surface to strain, disorder and vibrations in thiolcapped CdTe nanocrystals. J. Chem. Phys. **108**(18), 7807–7815 (1998)
44. Dundurs, J., Mura, T.: Interaction between an edge dislocation and a circular inclusion. J. Mech. Phys. Solids **12**(3), 177–189 (1964)
45. Dundurs, J.: Elastic interaction of dislocations with inhomogeneities. Math. Theory Dislocat, 70–115 (1969)
46. Smith, E.: The interaction between dislocations and inhomogeneities—I. Int. J. Eng. Sci. **6**(3), 129–143 (1968)